Numerical modeling of coated gratings in sensitive cases

Leonid I. Goray

International Intellectual Group, Inc., P. O. Box 335, Penfield NY 14526, USA
lig@pcgrate.com

Sergey Yu. Sadov

Institute for Problems in Mechanics, Rus. Acad. Sci., Moscow 117526, Russia
sadov@diffr.com

Abstract: Grating designs of practical interest, with subtle features of efficiency curves sensitive to the data or requiring very accurate computations, are considered. Examples (conformal and non-conformal coated gratings, in both polarizations) include: grating with a very thin oxide layer; non-conformal grating having a very narrow resonance peak, sensitive to refractive index measurements and interpolation; non-conformal sinusoidal grating with coating in the form of semi-cylinders with turn points; echelle with a tapered coating. The results are obtained by two integral method codes of the PCGrate$^{\mathrm{TM}}$ software. Implementation details and validation of results are discussed.
OCIS codes: 050.1950, 000.4430

1. Introduction

Many known rigorous methods for calculation of diffraction efficiencies of periodic relief gratings can, at least in principle, be applied to multilayer structures. Such applications have been reported for the differential method and the integral method [1], the modal method [2], the coupled waves method [3,4], the Chandezon coordinate transformation method enhanced by Li [5,6]. The simplest and most straightforward method is that of Rayleigh, but it works only under well-known restrictions on geometry of the layer boundaries [1]. Some of the methods can also benefit from special assumptions on geometry. In particular, it is always easier to deal with *conformal gratings*, i.e. multilayer gratings with all bounded layers being conformal. A *conformal layer* is a layer between two parallel boundaries, i.e. one of its boundaries can be brought onto another by a translation.

Among the above mentioned methods, only the integral one is capable to handle efficiency calculations in case of arbitrary grating geometry, any polarization, and in a broad range of period-to-wavelength (d/λ) ratios: from low resonance values $d/\lambda \sim 1$ up to hundreds, such as for echelles [7, 8], or for gratings working in the soft x-ray or in the VUV (vacuum ultra-violet) range [9], including real gratings with profile shapes obtained by measurements [10]. Rapid progress in super-smooth coating technology, together with requirements for broadening devices' working range and increasing sensitivity, have stimulated efforts on mathematical modeling of gratings with several conformal [11–13] and one non-conformal [14] thin layers. Further theoretical developments and

OSA TOPS Vol.75, Diffractive Optics and Micro-Optics
Robert Magnusson, ed.

numerical studies of more complicated gratings that have many non-conformal layers are interesting and practically important.

Although multilayer versions of the integral method have long been known (see e.g. a very clear exposition in [15]), the integral approach has not yet become popular in multilayer grating modeling. Indeed, writing, debugging and testing a multilayer integral code is a formidable task. Our effort on creating such a code, PCGrate-S, is announced here. In this paper we consider only gratings with single-layer coating (i.e. having two borders between different media). Examples of grating designs, chosen with potential applications in mind, demonstrate sensitive details of efficiency calculations, and mark limitations of our code. The examples embrace the whole spectral range, from infrared to VUV, gratings with thin and thick layers, dielectric and finitely conducting layers, and various geometry of borders.

The paper is organized as follows. In Sect. 2 we outline variants of the integral method used in commercial PCGrate^{TM} software, with an emphasis on their distinctive features. Related issues of accuracy and verification of results are touched. In Sect. 3, we proceed to the title subject — examples of efficiency calculations in sensitive cases. Some of them are meant to be "stress tests" for our code, while others demonstrate subtle, but potentially significant, features of efficiency curves, which may be easily overlooked.

These calculations were first reported at the DOMO Conference (Tucson, AZ, 2002) and published in an abridged form in [16].

2. Integral Method: features of implementation

A. Elements of the Integral Method

The essence of the integral method (or methods) is a reduction of a diffraction problem's dimension by one, which leads to a great time and memory saving in computations.

A self-contained exposition of this theory is well beyond this paper's scope. There are numerous good references, e.g. [1, 15, 17]. The integral method is so flexible that we can point out three *groups* of its "degrees of freedom". Purpose of this section is to specify particular choices and solutions used in our computer codes.

The three groups are:

- Mathematical structure: form of integral equations (choice of potentials), multilayer scheme;
- Methods of discretization, including treatment of corners (edges);
- Low-level details (calculation of the Green functions and their derivatives, solution of linear systems, detecting and cacheing of repeating intermediate quantities, etc.)

The term *modified integral method* used in publications ([13] and references therein) with regard to the PCGrate^{TM} software was introduced with this flexibility in mind. More precisely, it is meant to be "modifiable" or "tunable", however we keep the earlier term as a label. In a narrow technical sense, the modified integral method is characterized in Sect. 2C.

B. Multilayer grating solvers

Computations for this work were performed using two codes (solvers), PCGrate 2000 (in Sect. 3A), and a newer one, PCGrate-S. The former finds an approximate solution to a multistack problem

with thin layers using an integral equation on one boundary. The latter is not as fast, since it employs integral equations on all boundaries, but it does not rely on asymptotical assumptions.

PCGrate 2000. The multilayer solver of PCGrate 2000 is primarily intended for echelles with steep working facet or for very smooth profiles at 'x-ray' wavelengths.

In one of the first publications on multilayer integral method, Botten [18] considered a grating that contains one profile of arbitrary shape and several plane interfaces above and below it. Since the field values at adjacent plane interfaces are related by the known Fresnel coefficients, the whole multistack problem can be effectively reduced to one integral equation on the modulated profile. As the depth of modulation and the wavelength decrease, the problem with plane interfaces becomes a good approximation to the problem with conformal non-plane boundaries. This multilayer approximation works well in all practical cases in the x-ray range including the soft x-ray to EUV (extreme ultra-violet) wavelengths.

On the other hand, for echelles, in which the resonance on working facet plays a predominant role, it is often (but not always) possible to "rotate" the plane stack and consider a multilayer problem with the stack parallel to the working facet rather than to the substrate. Working facet angle for echelles usually exceeds 60 deg, so the Fresnel coefficients for the rotated stack differ significantly from those of the original stack. This approach generally works in case of thin layers (thickness-to-wavelength ratio $t/\lambda \le 1/10$), or even thick layers with a low modulation-to-wavelength ratio h/λ. Its applicability depends also on the absolute value of the difference $(\varepsilon_1 - \varepsilon_2)$ between the permittivities of the layer and the substrate, as well as on the period-to-wavelength ratio d/λ. A convenient rule of thumb is

$$(d/\lambda)|\varepsilon_1 - \varepsilon_2|(h/\lambda)(t/\lambda) \ll 1. \tag{1}$$

For the soft x-ray range gratings the left-hand side is a product of one big, one small, and two small to moderate values $(10^1 \div 10^3) \times (10^{-1} \div 10^{-3}) \times (10^0 \div 10^{-1}) \times (10^0 \div 10^{-2})$, so the criterion (1) is met almost always. In the presence of waveguide modes and other resonance peculiarities, this model, of course, is not valid.

PCGrate-S. This solver uses Variant D by classification in [15, Sect. 2]. Assuming that incident field is given on the upper side of the grating, a final integral equation with respect to an unknown convolution density on the upper boundary is obtained by solving a recurrent chain of integral equations on lower boundaries, starting from the bottom and moving upwards.

To our surprise, we found that a scheme suggested in [11] (for 2-layer case) works in the opposite direction and leads to a final equation with respect to an unknown convolution density on the lower boundary. Our experiments with that scheme (not related to computations reported in Sect. 3) showed its numerical instability. We offer a theoretical explanation below. It remains unclear to us how to make use of a program based on that scheme if the number of collocation points exceeds approximately 50.

Let us demonstrate the stability issue on a simple example. Consider a system of two weakly connected linear algebraic equations

$$\begin{pmatrix} D_1 & W_{21} \\ W_{12} & D_2 \end{pmatrix} \begin{pmatrix} \Phi_1 \\ \Phi_2 \end{pmatrix} = \begin{pmatrix} U \\ 0 \end{pmatrix}. \tag{2}$$

Weak connection means $|W_{12}|, |W_{21}| \ll 1$. Eliminating one of the unknowns Φ_1 or Φ_2, we obtain a single linear equation with respect to the remaining unknown.

Unstable scheme. Eliminating Φ_1 from the 2nd row of Eq. 2

$$\Phi_1 = -W_{12}^{-1} D_2 \Phi_2. \tag{3}$$

leads to the final equation with respect to Φ_2:

$$(-D_1 W_{12}^{-1} D_2 + W_{21})\Phi_2 = U. \tag{4}$$

In this scheme we refer twice to the inverse of a small number W_{12}, hence a loss of precision.

Stable scheme. We use again the 2nd row of Eq. 2, but now express Φ_2 via Φ_1:

$$\Phi_2 = -D_2^{-1} W_{12} \Phi_1. \tag{5}$$

The final equation w.r.t. Φ_1 reads

$$(D_1 - W_{21} D_2^{-1} W_{12})\Phi_1 = U. \tag{6}$$

No small denominator is encountered here.

"Small denominator" in the operator sense. Now suppose that Eq. 2 is a system of integral, rather than algebraic, equations, with D_1, D_2 being invertible integral operators with respect to a suitable pair of source and target function spaces, and the antidiagonal operators W_{ij} being "infinitely smoothing". Then W_{ij}^{-1} do not exist as bounded operators. A discretization of scheme (Eqs. 3,4) employs inversion of an ill-conditioned matrix that approximates the non-invertible operator W_{12}.

As applied to a diffraction problem with two boundaries, the situation is a bit more complex, since $\Phi_{1,2}$ become vector-functions that represents boundary data of a solution of the Helmholtz equation. The 2×2 system of vector integral equations is, in fact, a 4×4 system of scalar equations, but it is irrelevant to our discussion. The important fact is that operators connecting boundary data on *different* boundaries are always infinitely smoothing. In particular, such are operators $\mathcal{A}_2^-$, $\mathcal{B}_2^-$ in [11, Eq. 30]; thus the matrix inversion in Eq. 30 is an ill-conditioned operation. Contrary, neither of operator matrices that need to be inverted in any of the schemes in [15] is infinitely-smoothing.

C. Discretizations, options and parameters

Progress in algorithms for numerical solutions of one-dimensional integral equations in the last two decades has been nearly comparable with that of computer hardware. However, algorithms that possess superior convergence properties are less universal with respect to a scatterer geometry and not well-behaved in the high-frequency range. By these reasons, in the existing PCGrate codes, more classical and robust approaches are used. Numerical solution of integral equations is based on collocation with piecewise constant basis functions. The principal parameter, with respect to which the convergence is evaluated, is the number N of collocation points on each boundary. (In the actual program, N may vary from one boundary to another, which can be useful; see Sect. 3C. At present, let us discard this option for simplicity.)

Three basic sources of numerical error are: (a) replacement of an integral equation by a finite system of linear algebraic equations; (b) inexact evaluation of matrix elements; (c) inaccuracy of solution of the linear system.

Errors of type (c), as well as direct round-off errors, are neglectable provided the numerical scheme in use is stable and the problem "generic". Note that some methods, e.g. differential and

Rayleigh's, but not integral, inherently suffer from ill-conditionness as N or the wavenumber increases. Important though relatively rare non-generic, or degenerate, cases usually occur in studies of whole families of problems, rather than isolated ones. Examples include Wood's anomalies, very close boundaries, occasional isolated eigenvalues.

For errors of type (a), in many cases *a priori* estimations via functional-analytic and operator-theoretical methods are available, which, at least, can moderate one's optimistic expectations about the overall convergence rate. Errors of type (b) in collocation methods are commonly attributed to numerical quadratures. Combinations of collocation and quadrature methods with balanced convergence properties are known as quallocation methods. In periodic diffraction problems, in contrast to diffraction on a compact obstacle, there is one more source of (b)-type numerical error: evaluation of grating Green functions and their normal derivatives. The problem is seen from the well-known series representation (which we call, for brevity, the Green series), see e.g. [1, Eqs. 3.19, 3.20]. Convergence of the series deteriorates as the distance between the Green function's arguments (a collocation node and a quadrature node) tends to 0. The *modified integral method* in a narrow sense is a quallocation method that also specifies a summation rule for the Green series. In the simplest case, the series is truncated symmetrically at lower summation index $-P$ and upper index P; where P is an integer defined by

$$P \approx \kappa N. \tag{7}$$

The "truncation ratio" κ is optimized at small values of N and is kept constant as N increases. It has been found [19] that $\kappa = 1/2$ is a reasonably good choice for many practical computations.

Quadratures in our codes are performed by rectangular rule with single-term corrections: for the Green function - taking into account its logarithmic singularity [1, Eqs. 3.113, 3.114]; for the normal derivatives of the Green function - accounting for the profile curvature [1, Eq. 3.106]. For gratings with smooth boundaries, this method yields the overall error estimate $O(N^{-3})$ for diffraction amplitudes and efficiencies in both polarizations. However, the above simple truncation rule for the Green series is insufficient to match such accuracy of the quallocation. An easy remedy is provided by Aitken's δ^2 acceleration [20] applied to the truncated Green series. The precision of Aitken's method for individual values of the Green series, especially at close arguments, is inferior to that provided by the Kummer acceleration used in the IESMP code ([8] and earlier by Shestopalov et al., see [21)], or by the Euler method [21], but one would not benefit from an the extra accuracy in the end.

In presence of a profile with corners (piecewise linear), the profile's curvature can be formally described as a sum of δ-terms concentrated at the corners. Correspondingly, we use two versions of the quadrature formula involving the normal derivative of the Green function. (a) The collocation and quadrature nodes are set in such a way that all corners are nodes; the curvature corrections are replaced by corner terms according to [15, p. 120]. (b) The nodes are set in such a way that every corner lies half-way between the nodes adjacent to it; in this case, no curvature-like corrections are added. Both versions are found to yield approximately the same convergence rate $O(N^{-2+\varepsilon})$, where $0 < \varepsilon < 1$ apparently depends on the profile geometry.

In practice, the accuracy of results depends also on the distribution of collocation points. Better results are often obtained using the equidistant distribution along the arclength [8]. In case of "non-function", e.g. lamellar, profiles the parametrization by arclength is mandatory.

A note on the shortwave case. In case $\lambda/d \ll 1$, e.g. for echelles or x-ray gratings, introduction of any acceleration terms has an adverse numerical effect because of uncontrolled growth of coefficients

in "asymptotically enhanced" theoretical estimations. Treatment of such situations remains a kind of art. With all acceleration options turned off, it is often possible to obtain surprisingly good convergence of efficiencies at orders of practical interest, and the energy balance very close to 1.

D. Validation of results

Some computations presented in Sect. 3 are aimed to challenge our codes at their limits, so a few words regarding trustworthiness of the results are appropriate.

Workability of the programs has been confirmed in non-extreme cases by numerous tests, including: (a) the reciprocity theorem, (b) energy balance (generalized in the lossy case), (c) stabilization of results while doubling the number N of collocation points and varying the truncation ratio P/N, (d) comparison with analytically available case of plane interfaces, (e) considering the inverse (non-physical) radiation condition, (f) inserting fictitious boundaries with different geometric properties in a layer, (g) using different variants of collocation points distribution and shifts, and (h) comparing results to published ones, or obtained by our other programs, or corresponded to us by other researchers.

In complicated cases, a magnitude of the computational error can not be reliably deduced from accuracy criteria based on a single computation (such as the energy balance and the inverse radiation condition test). Much better are comparative studies, i.e. N-doubling or changing a configuration of collocation points. All results presented here, have been confirmed by one or another comparative tests, though some of the computations took a long time.

3. Numerical results

Refraction indexes for all our examples, except those corresponding to Fig. 3, are taken from [22], and interpolated by cubic splines between the reference values. Data from [22] earned a good reputation in calculations of multilayer structures in a broad spectral range, from EUV to FIR.

Computations were carried out on a Dual Intel® Pentium® III 1 GHz, 256 KB Cache Workstation with 512 MB RAM, 133 MHz Bus clock, working under MS Windows® 2000 Pro.

Light is incident from vacuum.

A. Grating with very thin oxide layer

Fig. 1 shows spectral dependencies of the absolute efficiency at the -1st autocollimation order in the VUV range for a sinusoidal aluminium grating 3600 grooves/mm, 100 nm depth, with conformal coating of different vertical thickness.

In this example, the minimal layer thickness $t = 0.25$ nm is comparable to atomic dimensions. In this case, the ratio t/λ is very small, while d/λ and h/λ are of order 1. According to the criterion (Eq. 1), this case can be successfully treated by the PCGrate 2000 code. Calculation of each point on Fig. 1 by PCGrate 2000 took less than a minute on above specified hardware, with $N = 400$ collocation points, which gave energy discrepancy 10^{-3} or better. An error in the -1th order efficiency measured by doubling N was of order 10^{-4}.

For the PCGrate-S code, this example was very hard, because of the small ratio t/d which lead to a close-to-singular behaviour of cross-boundary Green functions. In the most difficult case, $t = 0.25$ nm, obtaining three stable decimals in the -1th order efficiency required $N = 1750$ in TE polarization and $N = 2000$ in TM. Energy error was $\sim 10^{-5}$. With the truncation ratio $\kappa = 1/2$,

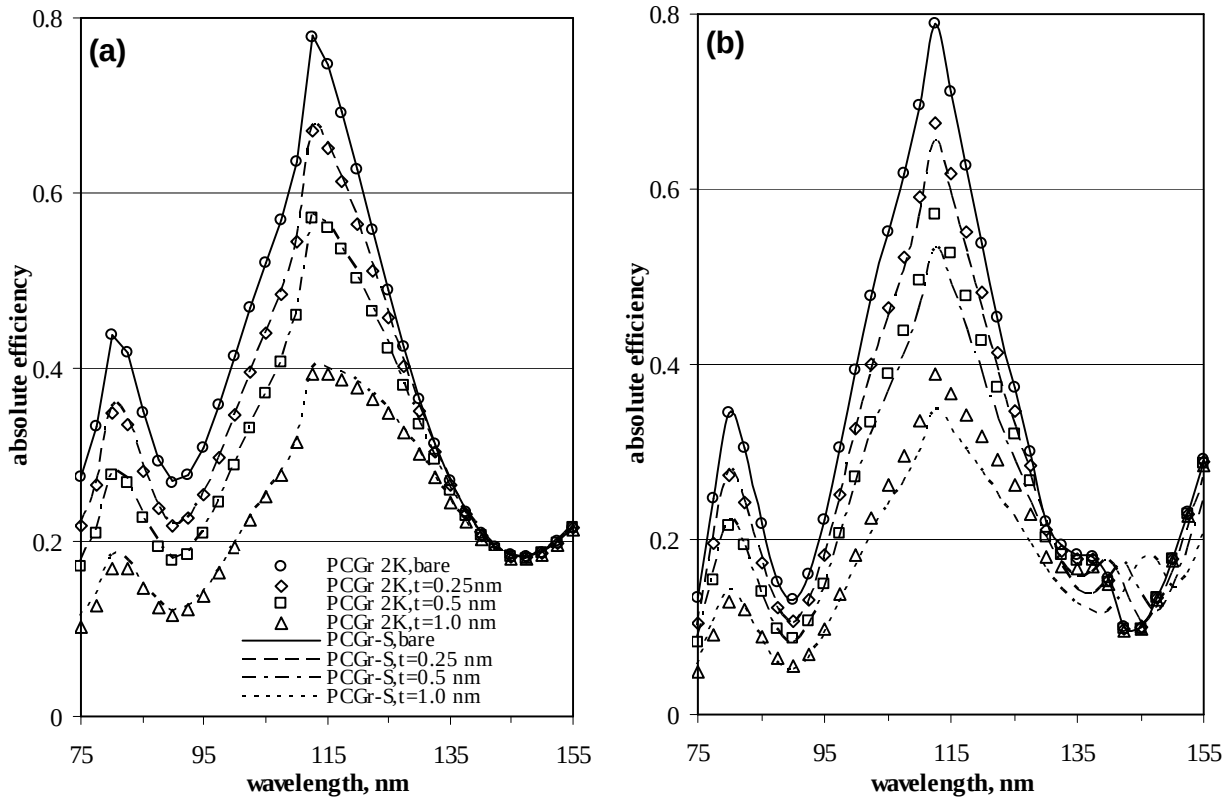

Fig. 1. Grating: 3600 gr/mm, sin, 100 nm depth, Al. Coating: Al_2O_3, thickness t. Mode: -1st Littrow order at $\lambda = 75 \div 155$ nm. (a) TE, (b) TM.

calculation of each point took several hours. As the thickness t increased, the number of collocation points for the same accuracy could be reduced in inverse proportion.

In TE polarization, the agreement of results obtained by both codes, is very good at any tried thickness. In TM, the agreement is very good for the bare grating and for the smallest thickness of coating $t = 0.25$ nm. We conclude that time and memory requirements of the exact solver (PCGrate-S) and the accuracy of the approximate multilayer solver (PCGrate 2000) are complementary to each other, which makes helpful to use them in combination.

Maximum discrepancy between results from the two solvers (about 8 absolute percent) is observed in TM polarization, at maximum layer thickness 1 nm, in the long wavelength part of the spectrum. Here is a plausible explanation. Because of considerable grating depth and big jumps of the refractive index, resonance phenomena in the oxide film, which interfere with PCGrate 2000's assumptions, begin to develop at a relatively small layer thickness. It is worth mentioning that PCGrate 2000's efficiencies in the "bad" region are almost independent on the layer thickness, i.e. nearly coincide with the efficiencies of the bare grating.

Results shown on Fig. 1 are interesting not just as an extreme computational exercise. Typical thicknesses of oxide coating that are investigated are some dozens nanometers [11,23]. Fig. 1 demonstrates that even a much thinner (by two decimal orders) oxide film diminishes reflectance of the aluminium grating near the absorption edge 110 nm by several times. A similar effect of

strong influence of an Al_2O_3 film with thickness just a few atomic sizes on the absolute efficiency of multilayer gratings has been studied earlier, theoretically and experimentally, in the far shorter wavelength ranges: soft x-ray and EUV [13].

B. Grating with thin coating: narrow anomalies

Figs. 2, 3 show spectral dependencies of the absolute efficiency at the -1st autocollimation order in the VUV range, TE polarization, for a sinusoidal aluminium grating of period $d = 300$ nm and depth $h_2 = 120$ nm, uncoated or coated by a MgF_2 layer with different thicknesses and sinusoidal upper surface of various depths h_1.

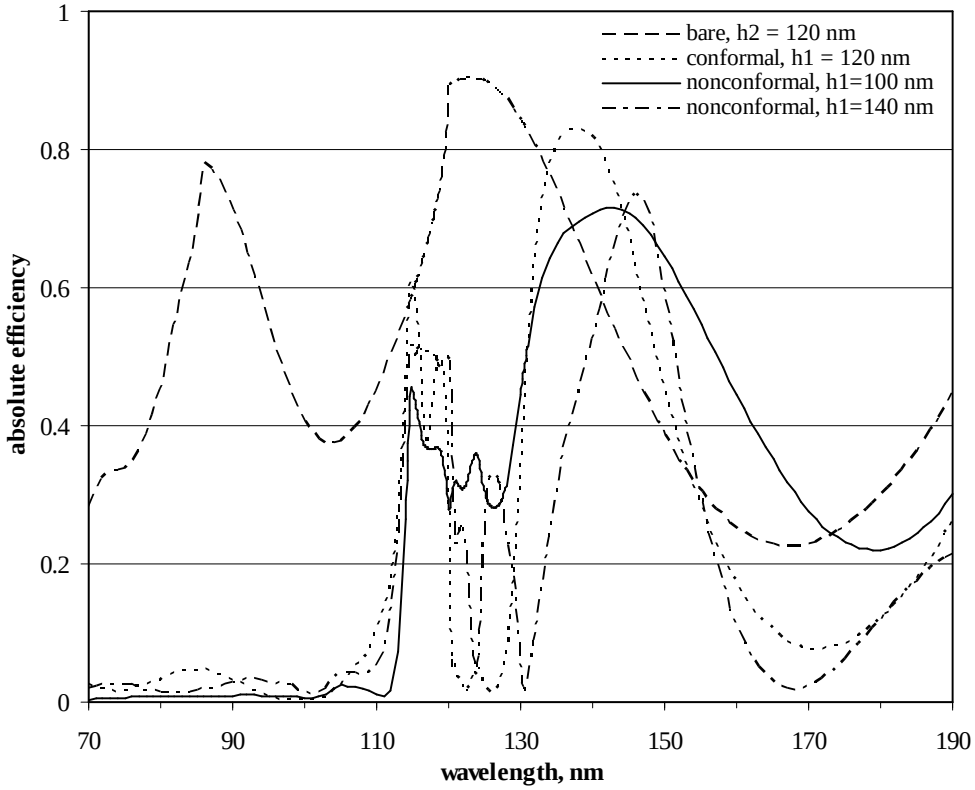

Fig. 2. Grating: $d = 300$ nm, sin, depth $h_2 = 120$ nm, Al. Coating: MgF_2, depth h_1. Mode: -1 Littrow order at $\lambda = 70 \div 190$ nm, TE.

Graphs on Fig. 2 correspond to the uncoated grating and three different coating shapes: conformal ($h_1 = h_2 = 120$ nm), non-conformal with thinner coating at the top ($h_1 = 100$ nm $< h_2$), and the opposite configuration, with thicker coating at the top ($h_1 = 140$ nm $> h_2$). Thickness of coating in the pits of the profile equals 25 nm in all three cases. Similar shapes of deposited layers are rather frequent in grating fabrication. The curve corresponding to $h_1 = 140$ nm is qualitatively resembling its sibling for the conformal coating, though positions and shapes of resonances differ. Contrary to that, the curve for $h_1 = 100$ nm is much smoother, without sharp gaps in the working range. Properties of non-conformal gratings like this could be exploited provided one were able to control the shape of non-conformal layers during fabrication.

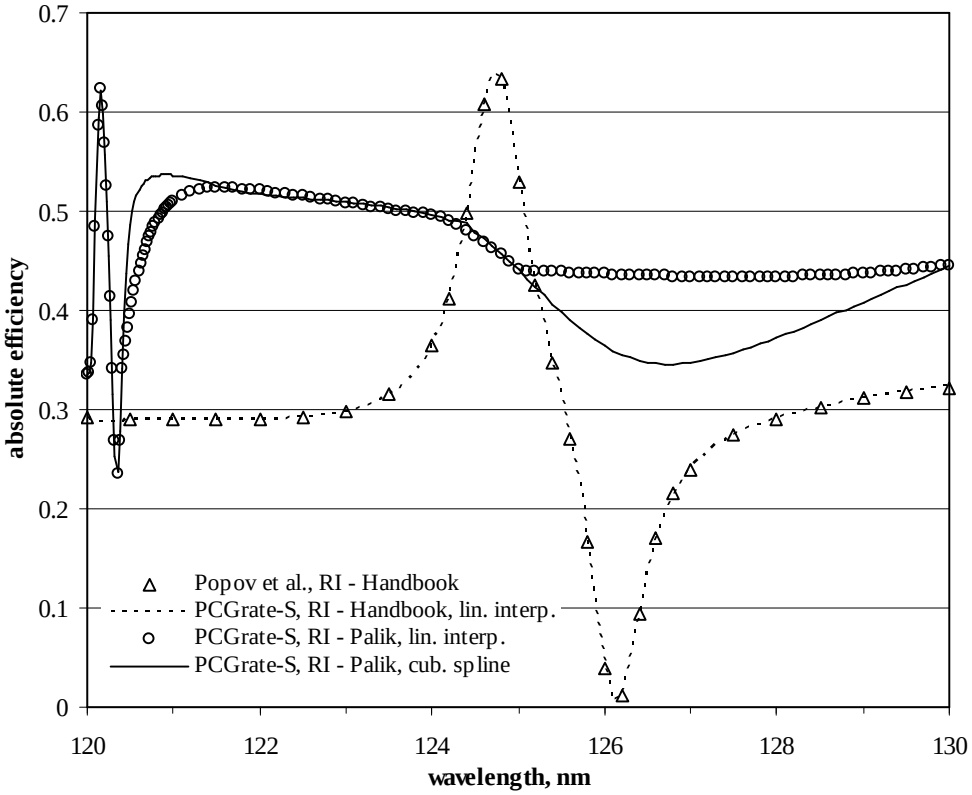

Fig. 3. Narrow and sharp anomalies for refractive indices of MgF_2 taken from different sources. Grating: same as on Fig. 2, conformal, $t = 50$ nm, at $\lambda = 120 \div 130$ nm.

Efficiency curves on Fig. 2 are calculated using the refraction index table from [22]. When using an older table from [24], the efficiency curves calculated with PCGrate-S (not shown) are identical, within graphical precision, to those from [11].

Graphs on Fig. 3 represent resonance peaks of efficiency, calculated at a high resolution in the range $120 \div 130$ nm, for a grating of the same type as previously (conformal, sinusoidal, $h_1 = h_2 = 120$ nm, vertical thickness 50 nm, coating MgF_2), with refraction indexes taken from two different sources [22], [24]. This example, on the one hand, demonstrates a very good agreement of our results with those published [11]. On the other hand, we see that not only positions and shapes of the resonances, but their very existence, depend on the data used. Origins and consequences of the uncertain knowledge of refractive indexes are discussed in detail in [7, Sect. 4A]. In our case, the half-width of the peak (and the gap) of the efficiency curve near $\lambda = 120.25$ nm, corresponding to data from [22], is only about 0.2 nm, which compares to typical half-widths of absorption lines of atoms in VUV [23]. In that small region, the real part of the refractive index undergoes a significant jump (Fig. 4), and diffraction orders -3 and $+2$ disappear to the right of $\lambda = 120$ nm. These peculiarities stipulate the appearance of a high resonance peak. As far as we know, such a narrow and deep resonance in the spectral characteristics of an "artificial" (as opposed to a crystalline) grating is revealed for the first time. On the efficiency curve corresponding to the data from [24], there exists a resonance near $\lambda = 125.5$ nm, which is absent on the former curve. The latter resonance's amplitude

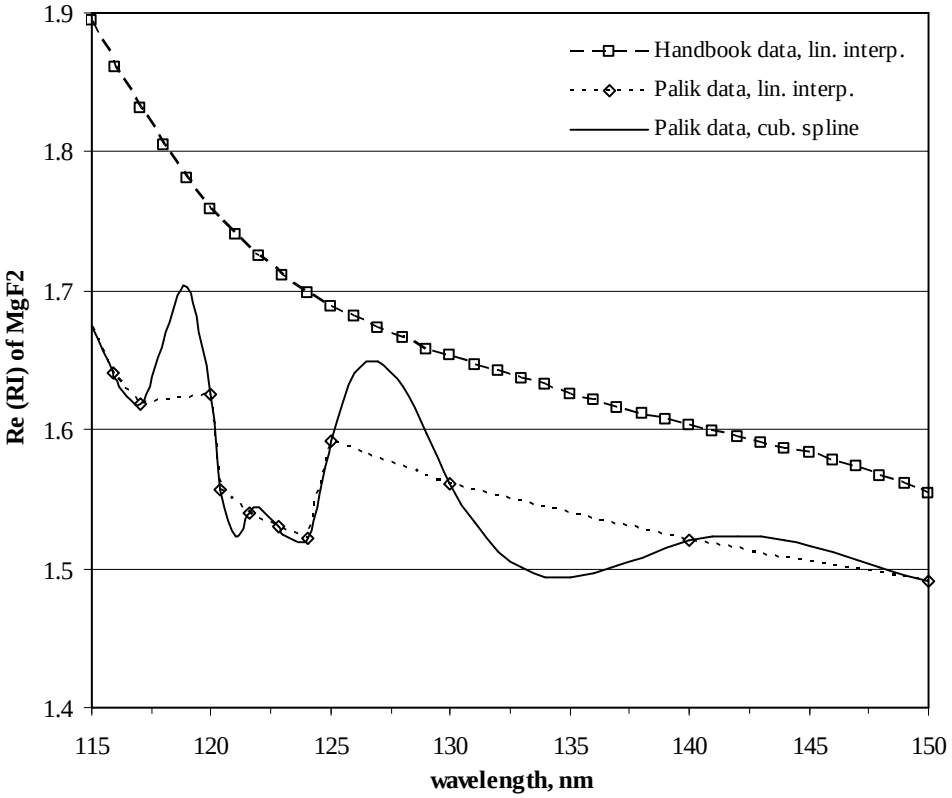

Fig. 4. Interpolated real part of MgF_2 refractive index from Refs. [22] and [24].

is only about twice as big as that of the former, but its width is almost order of magnitude bigger. Note also that a purely mathematical interpolation procedure has a visible effect on the efficiency curves e.g. near $\lambda = 127$ nm, where the interpolation-caused difference reaches about 9 absolute percent. This is due to the fast oscillation of data in the range $100 \div 130$ nm and low density of table data to the right of $\lambda = 125$ nm. The resonance near $\lambda = 120.25$ nm is not affected by the interpolation freedom, because there are enough interpolation nodes nearby.

Calculations for Figs. 2,3 are not too burdensome. Already on 100 collocation points, we achieve the energy error of $\sim 10^{-4}$. Efficiency correction at doubling the number of collocation points has the same order. Calculation of one point on the graphs required one to several seconds on the computer specified above.

C. Grating with thick nonconformal layer

In this example we consider a deep golden grating with 1000 grooves/mm, sinusoidal profile of depth $h = 500$ nm, covered by a dielectric layer of different shapes with refractive index 2. The grating works in the near infrared range $750 \div 1500$ nm, in the -1st autocollimation order, which is the only Bragg order existing under these assumptions.

The dielectric layer is either conformal, with vertical thickness 500 nm equal to the modulation depth, or non-conformal, formed by periodically, through $d/2 = 500$ nm, repeated semi-

cylinders. Maximum of the upper profile exceeds that of the lower profile also by 500 nm.

Big thickness of the layer in either case stipulates existence of waveguide modes that cause a strong energy redistribution in the spectral characteristics of the only existing order compared to the grating without coating. In the non-conformal case, the narrow "neck" around the semi-cylinder's turn point makes the process even more intricate.

Our results are presented on Fig. 5 (a,b). Dr. Lifeng Li kindly provided us results for comparison in the conformal and bare grating cases, calculated by the program *Delta*, which is based on the enhanced Chandezon method for multilayer conformal gratings [5]. Li's results are also shown on the figure. They agree with ours in 3–4 decimal places.

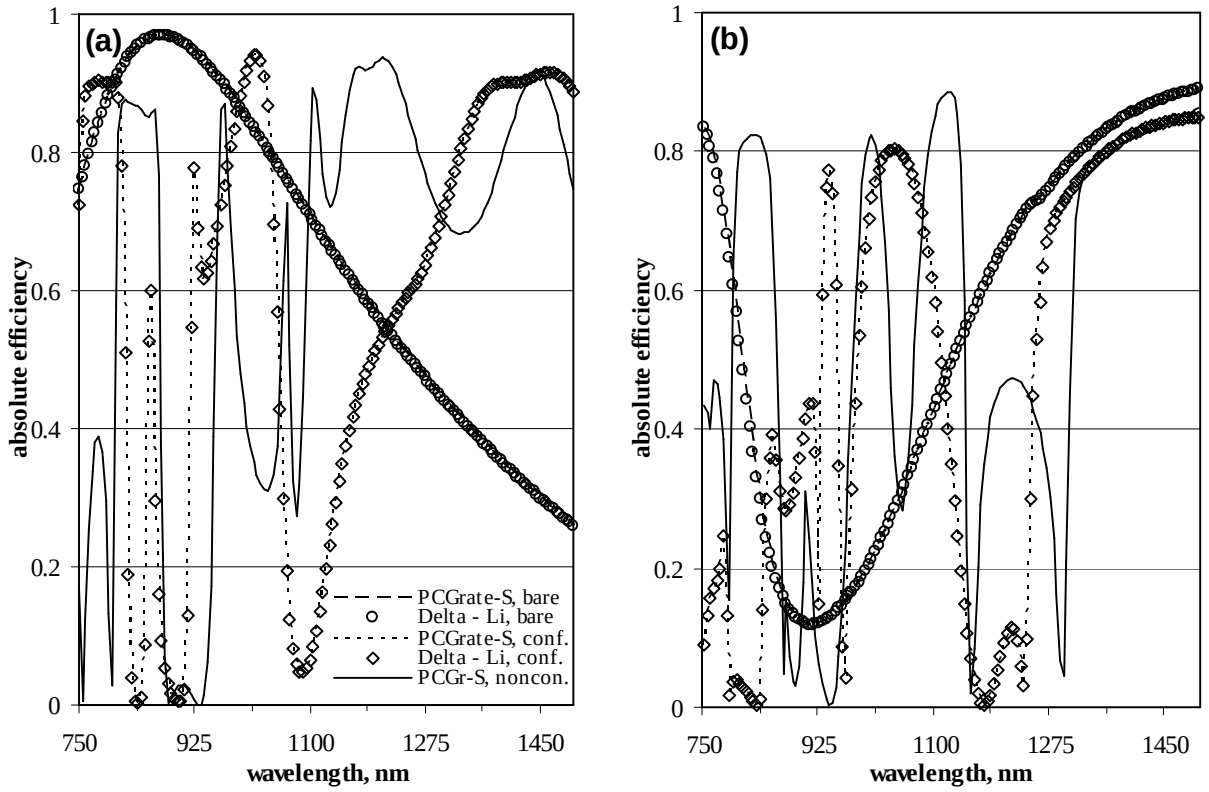

Fig. 5. Grating: 1000 gr/mm, sin, 500 nm depth, Au. Coating: dielectric $\nu = 2$, conformal or semi-cylindrical, $R = 500$ nm, $t \approx 500$ nm. Mode: -1st Littrow order at $\lambda = 750 \div 1500$ nm. (a) TE, (b) TM.

Behaviour of the grating with upper profile consisting of semi-cylinders has little in common not only with behaviour of the bare grating, but also with that of the conformally coated grating. It is quite interesting from theoretical and practical viewpoint. For instance, the absolute diffraction efficiency above approx. 70% in TE polarization survives in the wide range $1100 \div 1500$ nm (Fig. 5,a). In that range, the mean value of efficiency is about 82%. Such a wide and elevated efficiency "shelf" is not observed on other graphs on Fig. 5. In TM polarization, the non-conformal coating also yields a higher mean efficiency compared to the conformal case. Here again, like in the example of Sect. 3B, we encounter some potentially useful properties of non-conformal coatings.

For computations in this example, we used $N_1 = N_2 = 100$ collocation points on the sinusoidal profiles and $N_1 = 400 \div 800$ points on the semi-cylinder profile, which was approximated by the Fourier series with 25 harmonics. At the upper value of N_1, the energy error was almost everywhere 10^{-3} or better, while the deviation of efficiency at the -1st order was about 10^{-2} or better. Such a relatively poor accuracy is due to the field singularity near the turn points on the boundary. For sinusoidal modulation, the accuracy beat 10^{-3} already at $N_1 = 100$. Calculation of each point lasted from 1 sec. to 8 min.

D. Covered Echelle Grating

Echelles are among the most popular gratings, and at the same time among the most difficult for computations, especially those with dielectric coatings and working in the short wavelength range.

Our example in Sect. 3A shows that even a very thin oxide film on the grating surface may lead to deterioration of its reflectancy, at wavelengths < 130 nm. To avoid this, a thin ($10 \div 100$ nm) protection coating is applied on echelles' surfaces; usual material is MgF_2, but sometimes other dielectrics are used. At a certain thickness of the coating film, waveguide phenomena come out to affect the grating performance; as a result, the diffraction efficiency can either decrease or increase as compared to the non-oxidized bare grating. Non-conformal layers provide a new freedom in design, but the analysis of gratings becomes more complex.

Our last example deals with an aluminium echelle with 316 grooves/mm, working blaze angle 63.4 deg (r–2) and apex angle 90 deg. The grating works at the -47th order, TM polarization, and the wavelength $\lambda = 120$ nm. A protecting MgF_2 layer is applied. Consider three variants of its thickness and shape. In all variants the coating's upper boundary is a triangle with right angle at the top vertex, which is situated 30 nm above the grating's top vertex. The variants differ from each other by the coating's working angle, which is 63.4 deg (conformal case), or 62.9 deg, or 63.9 deg. Such a model of coating does not pretend to be the best description of a real structure formed by the coating, but it is simple and possible, and accounts for a deviation of coating direction from the substrate surface, which leads to a tapered shape on both slopes.

Fig. 6 presents angular dependencies of the grating efficiency. Also shown are results obtained with another integral method program, *IESMP* (Integral Equation System Method with Parametrization) [8, 14]. The latter results has been kindly provided by Dr. B. Kleemann.

All compared efficiency values agree in 3–4 decimal places in the conformal case and for bare echelle. Both codes, PCGrate-S and IESMP, treat the profile shape exactly, as a polygon, rather than using a trigonometric or a staircase approximation. Also in both codes the collocation points are distributed uniformly along the boundary w.r.t. arclength. The obtained agreement leaves little doubts about the accuracy of the corresponding curves.

In order to better understand possibilities of our program, we repeated the computations in the bare case and the conformal case using trigonometric representation of the profile instead. A good agreement of the efficiencies for the original and Fourier-approximated profiles for the bare grating is not surprising. However, it happens to be quite different in case of conformal coating, where the discrepancy at its maximum is about 6 absolute percent. We have enough evidence that it is not a convergence issue. The most puzzling fact is that the discrepancy is almost independent of the degree of trigonometric approximation. Corresponding curves on Fig. 6 refer to degrees 250 or 500, but the results are visually indistiguishable from those obtained with a degree $20 \div 30$. An explanation of this interesting phenomenon is yet to be found. It can be due to a combination of

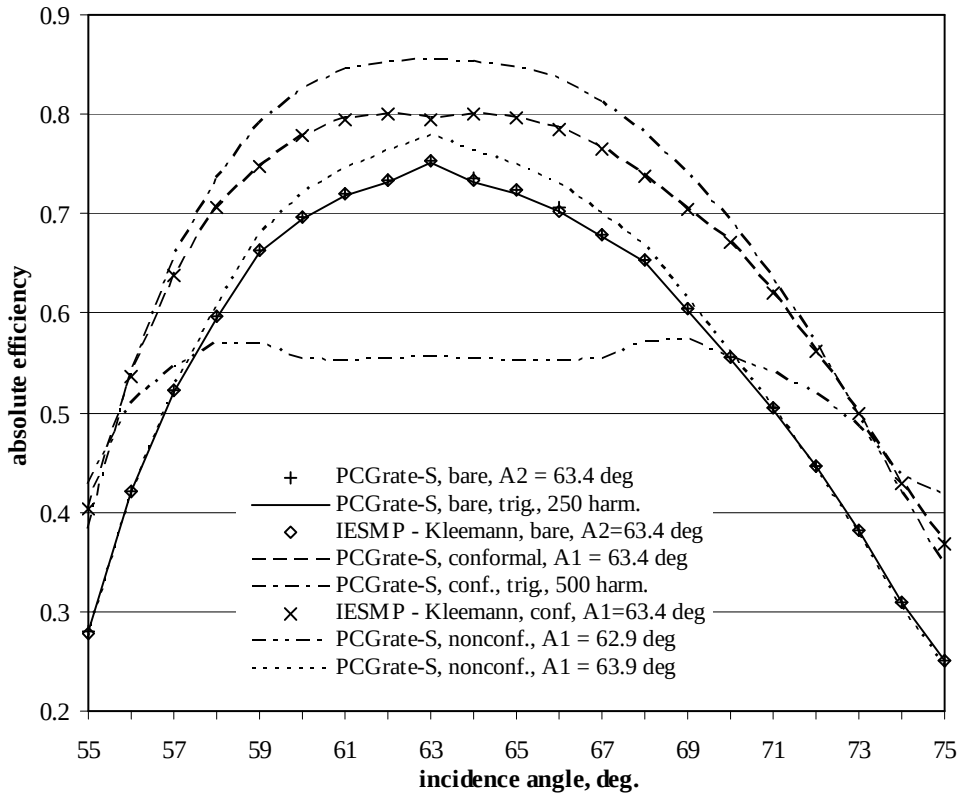

Fig. 6. Grating: 316 gr/mm, echelle r–2, working angle A1 = 63.4 deg, Al. Coating: MgF_2, $t = 30$ nm, conformal or nonconformal sawtooth. Mode: -47th order, TM, $\lambda = 120$ nm.

fast oscillations of the Fourier sums near the vertices and a resonance between two slopes of the coating.

Fig. 6 shows that the conformal coating leads to a noticeable increment of efficiency over the whole range of angles, by $\sim 10\%$ in average and 5% at the efficiency maximum. The non-conformal coating with working angle 63.9 deg also increases the efficiencies, but the effect is smaller and localized near the maximum. In contrast, the non-conformal coating with working angle 62.9 deg strongly reduces the efficiency at its maximum and leads to a practically flat efficiency graph. Geometry in this case is such that the working facet receives a thin layer of MgF_2, which narrows approaching the vertex; the idle facet gets a fatty coating. Such a model of non-conformal structure of real echelles has been proposed by experimentalists, who used it to explain significant loss of efficiency (G. Baccaro and S. Zheleznyak, private communications, 2001–02). Results of our computations admit this possibility. Efficiency of an echelle coated by such a non-conformal layer of MgF_2 can be 30–40% less than that of the uncoated grating in the whole central angular range. The efficiency is very sensitive to the deviation from conformal shape and to the vertical shift.

Computations in this example were carried out with $N = 200 \div 500$ for the bare grating and with $N = 400 \div 500$ for the coated conformal and non-conformal gratings. Error of the efficiency in the working order was less than 1%. In case of piecewise linear profiles many pairs of Green function arguments can be obtained from each other by translations; corresponding Green function values

are equal. There is an effective way to check for given arguments, whether we already encountered a congruent pair and calculated the Green function for it. This approach significantly reduces computational time for echelles, lamellar profiles, etc., and even more — in case of conformal layers, where the Green function values calculated on the upper side of the layer can be reused on the lower side. Calculation for each point on Fig. 6 required several seconds to several minutes.

Acknowledgments

We are grateful to the colleagues who provided some unpublished results, valuable comments and advises: Gary Baccaro, Bernd Kleemann, Lifeng Li, Evgeny Popov, and Semyon Zheleznyak.

References

1. R. Petit, ed. *Electromagnetic Theory of Gratings* (Springer-Verlag, 1980).
2. L. Li, "Multilayer modal method for diffraction gratings of arbitrary profile, depth, and permittivity", J. Opt. Soc. Am. A **10**, 2581-2591 (1993).
3. M. G. Moharam, D. A. Pommet, and T. K. Gaylord, "Stable implementation of the rigorous coupled-wave analysis for surface-relief gratings enhanced transmittance matrix approach", J. Opt. Soc. Am. A **12**, 1077-1085 (1995).
4. P. Lalanne, G. M. Morris, "Highly improved convergence of the coupled-wave method for TM polarization", J. Opt. Soc. Am. A **13**, 779-784 (1996).
5. L. Li, "Multilayer-coated diffraction gratings: differential method of Chandezon *et al.*, revisited", J. Opt. Soc. Am. A **11**, 2816-2828 (1994).
6. T. W. Preist, N. P. Cotter, and J. R. Sambles, "Periodic multilayer gratings of arbitrary shape", J. Opt. Soc. Am. A **12**, 1740-1748 (1995).
7. E. Lowen, D. Maystre, E. Popov, and L. Tsonev, "Echelles: scalar, electromagnetic, and real-groove properties", Appl. Opt. **34**, 1707-1727 (1995).
8. B. Kleemann, A. Mitreiter, and F. Wyrowski, "Integral equation method with parametrization of grating profile: theory and experiments", J. Mod. Opt. **43**, 1323-1349 (1996).
9. M. P. Kowalsky, J. F. Seely, L. I. Goray, W. R. Hunter, and J. C. Rife, "Comparison of the calculated and the measured efficiencies of a normal-incidence grating in the 125-225 Å wavelength range", Appl. Opt. **36**, 8939-8943 (1997).
10. D. Content, P. Arsenovic, I. Kuznetsov, and T. Hadjimichael, "Grating groove metrology and efficiency predictions from the soft x-ray to the far infrared," in *Optical Spectroscopic Techniques and Instrumentation for Atmospheric and Space Research IV*, A. Larar, M. Mlynczak, eds. Proc. SPIE **4485**, 405-416 (2001).
11. E. Popov, B. Bozhkov, D. Maystre, and J. Hoose, "Integral method for echelles covered with lossless or absorbing thin dielectric layers", Appl. Opt. **38**, 47-55 (1999).
12. J. F. Seely, L. I. Goray, W. R. Hunter, and J. C. Rife, "Thin-film interference effects of a normal-incidence grating in the 100-350 Åwavelength region", Appl. Opt. **38**, 1251-1258 (1999).
13. L. I. Goray and J. F. Seely, "Efficiencies of master, replica, and multilayer gratings for the soft x-ray–EUV range: modeling based on the modified integral method and comparison to measurements", Appl. Opt. **41**, 1434-1445 (2002).
14. B. Kleemann, R. Güther, "Metal gratings with dielectric coating of variable thickness within a period", J. Mod. Opt. **38**, 897-910 (1991).
15. A. Pomp, "The integral method for coated gratings: computational cost", J. Mod. Opt. **38**, 109-120 (1991).
16. L. I. Goray, S. Yu. Sadov, "Numerical modelling of nonconformal gratings by the modified integral method," in *Diffractive Optics and Micro-Optics,* Technical digest (OSA, Wash. DC, 2002), 41-43.
17. D. Colton, R. Kress, *Inverse Acoustic and Electromagnetic Scattering Theory* (Springer-Verlag, 1992).
18. L. C. Botten, "A new formalism for transmission gratings," Opt. Acta **25**, 481-499 (1978).
19. L. I. Goray, "Modified integral methods for weak convergence problems of light scattering on relief grating", in *Diffractive and Holographic Technologies for Integrated Photonic Systems*, R. I. Sutherland, D. W. Prather, and I. Cindrich, eds. Proc. SPIE **4291**, 1-12 (2001).

20. M. Abramowitz, I. Stegun, eds. *Handbook of mathematical functions* (Nat. Bureau of Standards, 1964).
21. M. A. Gilman, S. Yu. Sadov, A. S. Shamaev, S. I. Shamaev, "Computer simulation of scattering of electromagnetic waves: some problems associated with remote radar sensing of sea surface", *J. of Communications Technology and Electronics* **45**, Suppl. 2, 229-246 (2000).
22. E. D. Palik, ed. *Handbook on Optical Constants of Solids* (Academic, Orlando, FL, 1985).
23. J. A. R. Samson, *Techniques of Vacuum Ultraviolet Spectroscopy* (Pied Publ., Lincoln, NB, 1967).
24. American Institute of Physics, *Handbook* (McGraw-Hill, N.-Y., 1972).